JACS
JOURNAL OF THE AMERICAN CHEMICAL SOCIETY

Communication

pubs.acs.org/JACS

Mixing, Diffusion, and Percolation in Binary Supported Membranes Containing Mixtures of Lipids and Amphiphilic Block Copolymers

Douglas L. Gettel,[†,‡] Jeremy Sanborn,[§,‡] Mira A. Patel,[†] Hans-Peter de Hoog,[⊥] Bo Liedberg,[⊥] Madhavan Nallani,[⊥] and Atul N. Parikh*[,†,§,∥,⊥]

Departments of [†]Chemical Engineering & Materials Science, [§]Applied Science, and [∥]Biomedical Engineering, University of California, Davis, California 95616 United States

[⊥]Centre for Biomimetic Sensor Science, School of Materials Science & Engineering , Nanyang Technological University, Singapore 639798

Supporting Information

ABSTRACT: Substrate-mediated fusion of small polymersomes, derived from mixtures of lipids and amphiphilic block copolymers, produces hybrid, supported planar bilayers at hydrophilic surfaces, monolayers at hydrophobic surfaces, and binary monolayer/bilayer patterns at amphiphilic surfaces, directly responding to local measures of (and variations in) surface free energy. Despite the large thickness mismatch in their hydrophobic cores, the hybrid membranes do not exhibit microscopic phase separation, reflecting irreversible adsorption and limited lateral reorganization of the polymer component. With increasing fluid-phase lipid fraction, these hybrid, supported membranes undergo a fluidity transition, producing a fully percolating fluid lipid phase beyond a critical area fraction, which matches the percolation threshold for the immobile point obstacles. This then suggests that polymer-lipid hybrid membranes might be useful models for studying obstructed diffusion, such as occurs in lipid membranes containing proteins.

Fully synthetic polymer vesicles derived from high-molecular weight (M_W ~1500−20,000 g mol^{-1}), linear amphiphilic block copolymers, also known as polymersomes,[1] are proving to be mechanically tough and structurally robust alternatives to soft and flexible liposomes derived from discrete-length lipid amphiphiles (M_W ~600−1000 g mol^{-1}). Although equilibrium lyotropic phases of polymer amphiphiles, like those of lipids, typically consist of random mixtures of ordered mesophases (e.g., lamellar sheets, multilamellar vesicles, rods, and filaments),[2] uniform monodisperse populations of polymersomes can be readily obtained as kinetic (or metastable) configurations through an external input of energy. Specifically, by adapting methods based on mechanical extrusion, sonication, gentle hydration, and electroformation—developed originally for liposomes—unilamellar polymersomes over a wide range of sizes (50 nm to 50 μm) can be prepared.[1c,d,3] Moreover, planar supported polymer membranes can also be prepared by transfers of interfacial Langmuir monolayers from the air−water interface and by exploiting covalent and nonspecific interactions with the solid surfaces.[4]

In comparison with lipid membranes, polymer membranes exhibit superior mechanical stability and structural integrity.[5] They are characterized by (1) an improved ability to withstand large lateral strains (lower stretching moduli, 80−100 vs 250−1000 mN/m);[1c,5a] (2) reduced susceptibility to fluctuations and bending deformations (increased bending rigidity, 40−460 vs 10−30 K_BT);[5b] and (3) lower permeability coefficient for water (0.7−10 vs 15−150 μm/s).[5c] This robustness is a consequence of the longer hydrophobic core (8−30 vs 3−5 nm for lipid membranes), further augmented by the tunability of block lengths and the versatility in chemical structures of the monomers. The enhanced stability of polymersomes, however, comes with reduced lateral mobilities of polymer chains (0.01−0.1 vs 1−2 μm^2/s),[6] retention of which is critical if polymer membranes are to replicate the essential biophysical properties of their lipid counterparts.[6c] To this end, introduction of a fluid-phase colipid − producing mixed or hybrid lipid-polymer membranes − should afford a practical means to achieving a control over the balance between stability and fluidity.[7]

Here, we show that small hybrid vesicles (~100 nm diameter), consisting of lipids and block copolymers, in phosphate buffered saline (PBS, ~150 mM NaCl) fuse with solid surfaces, producing surface energy-dependent morphologies: bilayers form at hydrophilic surfaces, monolayers form at hydrophobic surfaces, and mixed monolayer/bilayer morphologies are obtained at amphiphilic surfaces. Moreover, the addition of a "fluidizing" colipid does not introduce large-scale phase separation in the resultant, mixed composition supported polymer-lipid membranes over a wide range of compositions. With increasing fluid-phase lipid fraction, these mixed membranes undergo a fluidity transition, producing a fully percolating fluid phase when the area fraction of the polymer component drops to (or below) a critical value, which matches with the critical, percolation threshold for point obstacles.[8]

We begin with the preparation of extended amphiphilic surfaces displaying predetermined, microscopic spatial patterns of hydrophilic and hydrophobic regions (Supporting Information (SI) Methods).[9] Briefly, hydrophobic OTS monolayers on glass are exposed to an ozone generating short-wavelength ultraviolet light (184−257 nm) in desirable patterns using a photomask. The treatment results in binary patterns of surface energy comprising of hydrophilic, oxidized silica in the UV-

Received: April 14, 2014
Published: July 8, 2014

dx.doi.org/10.1021/ja5037308 | J. Am. Chem. Soc. 2014, 136, 10186−10189

exposed regions surrounded by a hydrophobic OTS in UV-protected regions. The resulting amphiphilic surfaces are then incubated with aqueous phase dispersions in PBS of hybrid vesicles consisting of mixtures of a fluid-phase phospholipid, POPC (T_m = −2 °C) and PBD_{22}-PEO_{14} (M_W 1.8 kDa). The polymer has the ratio of hydrophilic to total mass, $f_{hydrophilic}$ = 33%, which falls in the range (29%−39%) suitable for vesicle formation[1c] and a low glass transition temperature (T_g, −10 °C), which ensures ready dispersion and mixing with lipids in aqueous media.[1a]

A combination of epifluorescence microscopy (Figure 1c,d) and imaging ellipsometry (Figure 1b) measurements confirm

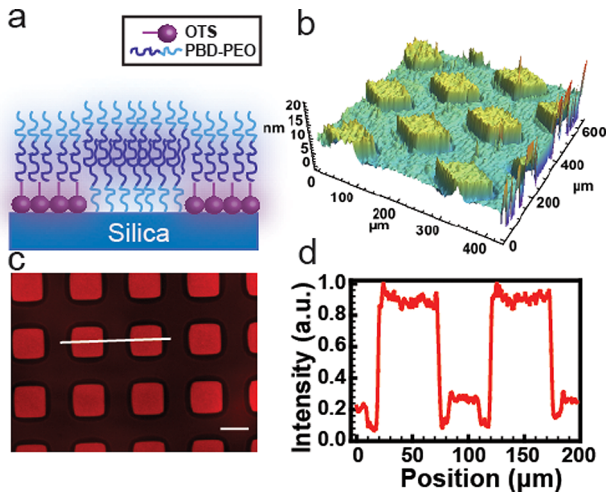

Figure 1. Substrate-mediated fusion of polymersomes. (a) Cartoon illustration of mono- and bilayer PBD-PEO morphologies obtained on hydrophobic and hydrophilic (squares) regions of the amphiphilic substrate pattern. (b) An ellipsometric height map for PBD-PEO patterns. (c,d) An epifluorescence micrograph and an intensity profile. Scale bar, 50 μm.

the rupture of nominally single-component pure polymersomes forming a well-defined, laterally contiguous, planar polymer membrane consisting of single bilayers, 10−12 nm in thickness, in hydrophilic regions and monolayers (5−6 nm thick) in hydrophobic regions (Figure 1a,b), and in good correspondence with surface-energy dependent fusion of phospholipid vesicles[9a,10] and polymer micelles.[9b] Moreover, fluorescence recovery after photobleaching (FRAP) measurements confirm the essential absence of long-range lateral fluidity (D < 0.1 $\mu m^2/s$) of supported polymer membranes (Movie S3.1.1) at room temperature.

This anomalously low diffusion constant,[6b] despite the fact that segment molecular weights of the BD and EO are below their corresponding bulk entanglement values ($M_{e,BD}$ = 3.5 kDa and $M_{e,EO}$ = 1.7 kDa), suggests that nominal Rouse-type polymer mobilities might be complicated by contributions from reptation-type motion[5d,6a] and/or frictional coupling of the hydrophilic EO units with the underlying substrate.[8d]

Substituting single component polymersomes with those derived from polymer-lipid mixtures (P/L molar ratios: 0/100, 5/95, 10/90, 18/82, 24/76, 49/51, 74/26, and 100/0) generates a self-consistent set of bilayer/monolayer morphologies on patterned surfaces. In all cases, despite a mismatch in core thicknesses of polymer and lipid, optically uniform fluorescence images are observed (Figure S2.1). This conspicuous absence of optically discernible lateral phase separation—at variance with large-scale phase separation observed in free membranes of comparable giant lipid-polymer vesicles[3,7a]—provides a clue for the substrate-mediated fusion mechanism: surface rupture of isolated lipid-polymer vesicles deposits immobile polymers, which become irreversibly adsorbed to the surface, at the "granularity" of the area of individual vesicles, thus stabilizing a submicroscopically uniform spatial distribution of polymer obstacles in the supported membrane disks. Subsequent fusion at the edges then produces a laterally contiguous supported membrane in direct analogy with substrate-mediated fusion of lipid vesicles.[10] A consequence of this imposed mixing of polymers and lipids is that localized depositions of multiple populations of polymer vesicles stabilize compositional gradients on single substrates (Figure S2.2). Another consequence of mixed character of polymer-lipid supported membranes is that the polymer component imparts a significant tolerance to drying: we found that as little as 10 mol% polymer is sufficient to stabilize hybrid supported membranes against damage caused by drying and air-exposure (Figure S2.3).

The regularly spaced distribution of immobile polymer then acts as a field of obstacles around which lateral diffusion of the lipid must occur. The ensuing anomalous diffusion, governed by percolation theory, suggests that for the long-range diffusion, the area fraction of the obstacles (C) must drop to (or below) the percolation threshold ($C < C_p$), defined as the highest concentration of point obstacles at which an infinite cluster of percolating fluid phase exists.[8b,e] Thus, elevating the relative concentration of the well-mixed colipid should afford long-range lateral fluidity in polymer membranes. To test this possibility, we examined lateral diffusion rates of a fluorescently labeled probe lipid or probe polymer (Figures S2.4−2.6) in supported membranes consisting of systematically varied binary mixtures of polymers and lipids using FRAP (Movies S3.1.1−S3.1.8 and S3.2.1−S3.2.8).

These results (Figure 2) confirm the onset of lateral fluidity at a critical lipid concentration, c_L of ∼74% (or c_p ∼26%), beyond which the probe diffusion constant climbs rapidly, increasing by over 2 orders of magnitude (with corresponding

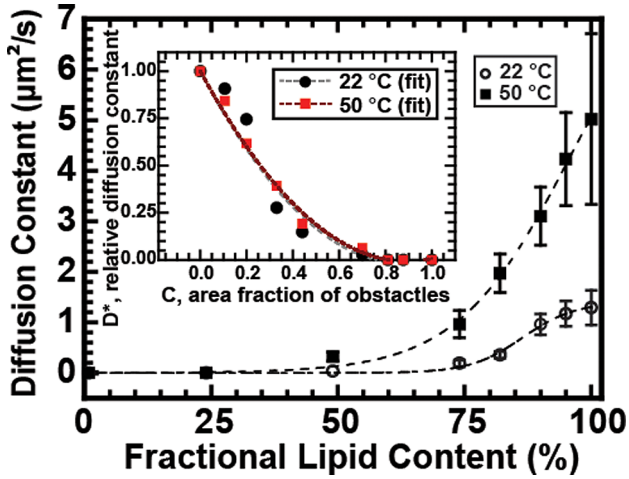

Figure 2. (a) Composition-dependent diffusion constants of probe lipid in mixed polymer-lipid supported membranes at 22 and 50 °C. Inset, dependence of the relative diffusion constant on area fraction of polymer obstacles. Fit to the modified free-area model: (1) a = −2.33 ± 0.23 and b = 1.34 ± 0.27 for 22 °C and (2) a = −2.26 ± 0.09 and b = 1.27 ± 0.10 for 50 °C (see Figure S2.7).

dx.doi.org/10.1021/ja5037308 | J. Am. Chem. Soc. 2014, 136, 10186−10189

increase in mobile fraction) producing a fully percolating fluid phase. Assuming the molecular areas of 1.5 nm^2 (a_p) and 0.68 nm^2 (a_L) $molecule^{-1}$ for the PBD-PEO[5d] and POPC,[11] respectively, the observed critical obstacle concentration of 26% translates into the threshold area concentration of polymer obstacles, C ($= a_p n_p/(a_p n_p + a_L n_L)$, where n_L and n_p represent the molar fractions of lipid and polymer respectively), of ~0.44. This value is in the range of values predicted from Monte Carlo simulations for 2D precolation thresholds on the triangular (C_p =0.5), the square (C_p =0.41), and the random (C_p =0.332) lattices[8b] and matches well with previous experiments in comparable systems.[8c,d]

Elevating the temperature to 50 °C increases the diffusion constants for all obstacle densities and elevates the apparent C_p to >0.7, likely caused by the transformation of immobile polymers into mobile obstacles (Movie S3.2, Figure S2.4–2.6). Although the percolation threshold must strictly vanish for mobile obstacles allowing long-range diffusion at all concentrations, experimental time scales make it difficult to measure low diffusivities (<0.05 $\mu m^2/s$) at high polymer concentrations.[12] Further, plotting the observed diffusion constants in terms of relative diffusion constant, D^*, defined as the ratio of diffusion constant in the presence and absence of polymer obstactles ($= D_c/D_0$) as a function of C, reveals that the profile for the two temperatures overlap (Figure 2, inset). This suggests that the effect of obstacle density scales with the fluidity of the mobile phase. Further analyzing these results using the modified free-area model,[8c] which includes the soft-core repulsion due to the ordering of boundary lipids in terms of a characteristic coherence length ξ yields $R/\xi = 1.9 \pm 0.2$ for the obstacles of average radius R. This translates into an annular rim of roughly 1 lipid size (Figure S2.7), which is close to ξ for proteins of comparable MW (e.g., gramicidin, 2 kDa).[8b,c] Taken together, the diffusional behavior of lipid-polymer supported membranes then offers a model configuration for studying the so-called "archipelago effect," obstruction of diffusion by immobile (or mobile) obstacles, such as occurs in membranes containing lipopolymers or proteins.[12]

Lastly, we consider whether the constraint on lipid polymer phase separation, imposed by limited polymer mobilities, can be circumvented to produce microscopically separated, long-lived lipid and polymer patches in single samples.[13] This is achieved by implementing direct patterning techniques, developed previously for supported phospholipid membranes[14] (Figure 3). Specifically, we find that a two-step process, involving fusion of single component polymersomes, followed by direct photopatterning and backfilling, can be readily implemented to produce engineered patterns of lipid and polymer components of arbitrary shapes and sizes.

Here, the primary process involves the fusion of single-component PBD-PEO vesicles onto uniformly hydrophilic substrate producing single, laterally contiguous polymer bilayers. Subsequent exposure in either wet or dry conditions to ozone-generating, short-wavelength UV light (187–254 nm) through a patterned photomask produces spatial patterns of polymer-free voids within the supported polymer bilayer, which are then "backfilled" by secondary fusion of POPC vesicles at the bared substrate producing long-lived and most likely metastable separation of fluid lipid and polymer bilayer regions (Movie S3.3) within single hybrid supported membranes.

In summary, results presented here show that substrate-mediated fusion of polymersomes (and their hybrid variants with colipids) is strongly dependent on local surface energy producing patterns of supported membrane morphologies at mixed wettability surfaces. In hybrid vesicles, the presence of fluid-phase lipid produces a microscopically mixed phase, which introduces long-range lateral fluidity above the percolation threshold for point obstacles. This then suggests that mixed lipid-polymer vesicles might be useful models for studying obstructed diffusion, such as occurs in cellular membranes, containing proteins of low mobilities.

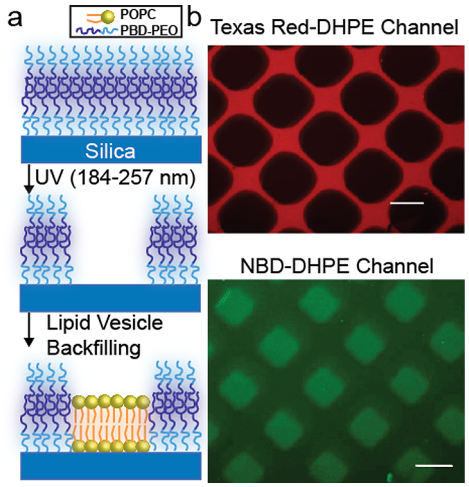

Figure 3. Engineered separation of lipids and polymers in supported membranes. (a) Cartoon illustrating selective removal and backfilling of patches of PBD-PEO bilayers with POPC bilayer. (b,c) Epifluorescence micrographs of PBD-PEO (containing TR-DHPE) and POPC (containing NBD-DHPE) bilayers, respectively. Scale bar, 100 μm.

■ ASSOCIATED CONTENT

Supporting Information

Detailed methods and characterization, figures, and movies. This material is available free of charge via the Internet at http://pubs.acs.org.

■ AUTHOR INFORMATION

Corresponding Author

anparikh@ucdavis.edu

Author Contributions

‡These authors contributed equally.

Notes

The authors declare no competing financial interest.

■ ACKNOWLEDGMENTS

We thank T. Wilkop for help with initial expertiments. This work is supported by a grant from Basic Energy Sciences, Department of Energy (no. DE-FG02-04ER46173).

■ REFERENCES

(1) (a) Zhang, L. F.; Eisenberg, A. *Science* **1995**, *268*, 1728–1731. (b) Discher, B. M.; Won, Y. Y.; Ege, D. S.; Lee, J. C. M.; Bates, F. S.; Discher, D. E.; Hammer, D. A. *Science* **1999**, *284*, 1143–1146. (c) Discher, D. E.; Eisenberg, A. *Science* **2002**, *297*, 967–973. (d) Antonietti, M.; Forster, S. *Adv. Mater.* **2003**, *15*, 1323–1333. (e) van Dongen, S. F. M.; de Hoog, H. P. M.; Peters, R.; Nallani, M.; Nolte, R. J. M.; van Hest, J. C. M. *Chem. Rev.* **2009**, *109*, 6212–6274.
(2) (a) Jain, S.; Bates, F. S. *Science* **2003**, *300*, 460–464. (b) Blanazs, A.; Armes, S. P.; Ryan, A. J. *Macromol. Rapid Commun.* **2009**, *30*, 267–277.

(3) (a) Nam, J.; Beales, P. A.; Vanderlick, T. K. *Langmuir* **2011**, *27*, 1−6. (b) Nam, J.; Vanderlick, T. K.; Beales, P. A. *Soft Matter* **2012**, *8*, 7982−7988.
(4) (a) Dorn, J.; Belegrinou, S.; Kreiter, M.; Sinner, E. K.; Meier, W. *Macromol. Biosci.* **2011**, *11*, 514−525. (b) Kowal, J.; Zhang, X. Y.; Dinu, I. A.; Palivan, C. G.; Meier, W. *ACS Macro Lett.* **2014**, *3*, 59−63.
(5) (a) Le Meins, J. F.; Sandre, O.; Lecommandoux, S. *Eur. Phys. J. E: Soft Matter Biol. Phys.* **2011**, *34*, 17. (b) Bermudez, H.; Hammer, D. A.; Discher, D. E. *Langmuir* **2004**, *20*, 540−543. (c) Lorenceau, E.; Utada, A. S.; Link, D. R.; Cristobal, G.; Joanicot, M.; Weitz, D. A. *Langmuir* **2005**, *21*, 9183−9186. (d) Srinivas, G.; Discher, D. E.; Klein, M. L. *Nat. Mater.* **2004**, *3*, 638−644.
(6) (a) Battaglia, G.; Ryan, A. J. *J. Am. Chem. Soc.* **2005**, *127*, 8757−8764. (b) Lee, J. C. M.; Santore, M.; Bates, F. S.; Discher, D. E. *Macromolecules* **2002**, *35*, 323−326. (c) Kusumi, A.; Nakada, C.; Ritchie, K.; Murase, K.; Suzuki, K.; Murakoshi, H.; Kasai, R. S.; Kondo, J.; Fujiwara, T. *Annu. Rev. Biophys. Biomol. Struct.* **2005**, *34*, 351−378.
(7) (a) Le Meins, J. F.; Schatz, C.; Lecommandoux, S.; Sandre, O. *Mater. Today* **2013**, *16*, 397−402. (b) Lim, S. K.; de Hoog, H. P.; Parikh, A. N.; Nallani, M.; Liedberg, B. *Polymers* **2013**, *5*, 1102−1114. (c) Kaufmann, S.; Borisov, O.; Textor, M.; Reimhult, E. *Soft Matter* **2011**, *7*, 9267−9275.
(8) (a) Coelho, F. P.; Vaz, W. L.; Melo, E. *Biophys. J.* **1997**, *72*, 1501−1511. (b) Saxton, M. J. *Biophys. J.* **1994**, *66*, 394−401. (c) Almeida, P. F. F.; Vaz, W. L. C.; Thompson, T. E. *Biochemistry* **1992**, *31*, 7198−7210. (d) Deverall, M. A.; Gindl, E.; Sinner, E. K.; Besir, H.; Ruehe, J.; Saxton, M. J.; Naumann, C. A. *Biophys. J.* **2005**, *88*, 1875−1886. (e) Skaug, M. J.; Faller, R.; Longo, M. L. *J. Chem. Phys.* **2011**, *134*, Art. No. 215101.
(9) (a) Howland, M. C.; Sapuri-Butti, A. R.; Dixit, S. S.; Dattelbaum, A. M.; Shreve, A. P.; Parikh, A. N. *J. Am. Chem. Soc.* **2005**, *127*, 6752−6765. (b) Goertz, M. P.; Marks, L. E.; Montano, G. A. *ACS Nano* **2012**, *6*, 1532−1540.
(10) Cremer, P. S.; Boxer, S. G. *J. Phys. Chem. B* **1999**, *103*, 2554−2559.
(11) Kucerka, N.; Tristram-Nagle, S.; Nagle, J. F. *J. Membr. Biol.* **2005**, *208*, 193−202.
(12) Saxton, M. J. *Biophys. J.* **1989**, *56*, 615−622.
(13) Zhang, H. Y.; Hill, R. J. *J. R. Soc. Interface* **2011**, *8*, 127−143.
(14) Yee, C. K.; Amweg, M. L.; Parikh, A. N. *J. Am. Chem. Soc.* **2004**, *126*, 13962−13972.